Supporting Information

A General Approach to Fabricate Free-standing Metal Sulfides@Carbon Nanofiber Network as Lithium Ion Battery Anodes

Ling Fei, Brian Patrick Williams, Sang Ha Yoo, Joe Michael Carlin and Yong Lak Joo*
School of Chemical and Biomolecular Engineering, Cornell University, Ithaca, NY 14853, USA
E-mail: ylj2@cornell.edu

Experimental Section

Synthesis of the metal sulfides@CNFs nanocomposites

To prepare the metal sulfides@CNFs, 2.3 mmol of metal acetates ($Co(CH_3COO)_2$, $Fe(CH_3COO)_2$, $Cu(CH_3COO)_2$, $Sn(CH_3COO)_2$ $Ni(CH_3COO)_2 \cdot 4H_2O$, $Mn(CH_3COO)_2 \cdot 4H_2O$) were thoroughly dissolved in 10% polyacrylonitrile (PAN) solution (0.5g PAN in 5g dimethylformamide). Then, 0.2g sulfur powder (Spectrum chemical MFG, Corp, SEM image in Fig S1) was well dispersed in the solution via untrasonication and magnetic stirring. Once the solution was ready, the electrospinning was carried out under ambient conditions using a Harvard Apparatus PHD 2000 Infusion syringe pump at a working voltage of 17.5 kV, working distance of 15 cm, and feeding rate 15μL min^{-1}. After electrospinning, the metal acetate/sulfur/PAN nanofibers webs were taken off the grounded aluminum foil for thermal treatment. Metal sulfides@CNFs were obtained by treating the as-spin fresh fibers at 700°C in N_2 for an hour with a heating rate of 5° C/min.

Characterization: The structure, composition, and morphology of the samples were characterized by X-ray diffraction (XRD, Scintag-Theta-Theta-X-ray-Diffractometer Cu Kα (λ = 1.5406Å) radiation, 40 kV/40 mA current), transmission electron microscopy (TEM; FEI-T12-Spirit-TEM-STEM, High-resolution TEM by Fei-F20Tecnai), and scanning electron microscopy

(SEM, Tescan-Mira3-FESEM) equipped with energy-dispersive X-ray analysis (EDX). The component ratio was decided by thermogravimetric analysis (TA instruments Q500). The X-ray photoelectron spectroscopy (XPS) was measured by Surface Science Instruments SSX-100. Electrochemical measurements were conducted using CR-2032 coin cells. The working electrodes were directly cut from the as-prepared fiber mats. A lithium foil was used as the counter electrode and a mixture of 1 M $LiPF_6$ in ethylene carbonate (EC)/dimethyl carbonate (DMC) (1:1 by volume) was used as the electrolyte. Cell assembly was carried out in an argon-filled glovebox with oxygen concentration below 1 ppm. The galvanostatic charge/discharge measurements were performed using a MTI battery testing system in the voltage window of 0.01-3 V (vs. Li+/Li). Cyclic voltammetry were measured using a PARSTAT 4000(Princeton Applied Research) electrochemical workstation.

SEM of Sulfur Precursor

As shown in Fig. S1, the sulfur precursor have irregular shapes and with size varying from 10μm to more than 100 μm.

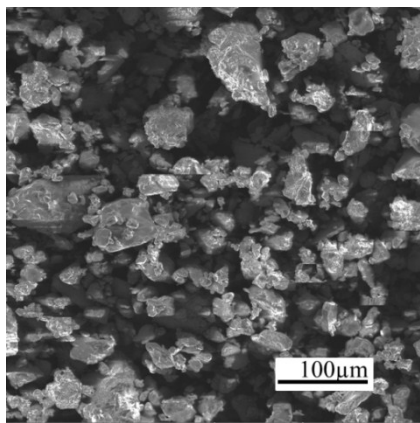**Figure S1** SEM image of sulfur particles.

XPS Analysis of Metal Sulfides@Carbon Nanofibers

XPS measurement for all samples has been conducted and shown in Fig. S2. The spectra show obvious characteristic peaks of Fe 2p, Mn 2p, Co 2p, Ni 2p, Cu 2p, Sn 3d, and S 2p. And S2p can be deconvoluted to S $2p_{3/2}$ and $2p_{1/2}$ with the spin-orbit separation of 1.16eV. All S $2p_{3/2}$ values are lower than that of elemental sulfur 164.0eV, confirming S exists in compound. The slight shift of peak values is due to the different binding metal ions around sulfur. Overall, the specific binding energy for both metallic phases and sulfur in all the materials are in good agreement with NIST XPS data base (September 15, 2012, National Institute of Standards and Technology) and previous reports.[1-5,28]

In the case of NixS@CNFs, the Ni $2p_{3/2}$ spectrum shows peak around 852.9eV, which could be assigned to either Ni^{2+} of NiS (853.1 eV) , metallic Ni (852.6 eV), or both, due to the difference between the binding energy of Ni^{2+} in NiS and metal Ni is very small (0.5 eV). The peaks at 162.51 eV and 163.67 eV are also present, and can be assigned to the binding energies of S $2p_{3/2}$ and S $2p_{1/2}$ of S^{2-}. With the presence of sulfur, the presence of NiS can be confirmed. This results is similar to literature report.[28] Additionally, Ni metallic phase has been identified from XRD analysis, therefore, the Ni $2p_{3/2}$ could be from the coexistence of Ni^{2+} and Ni metallic phase.
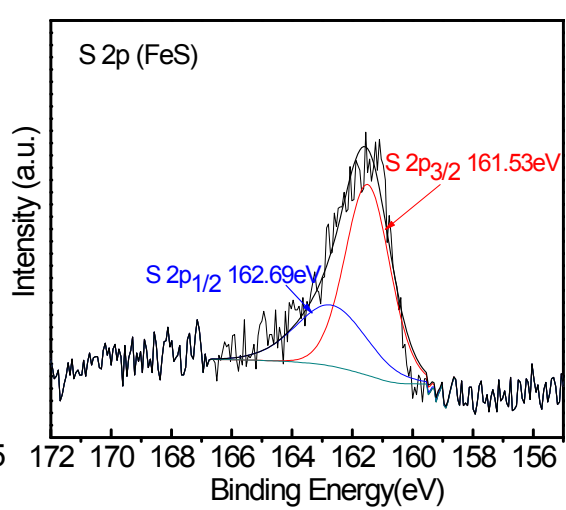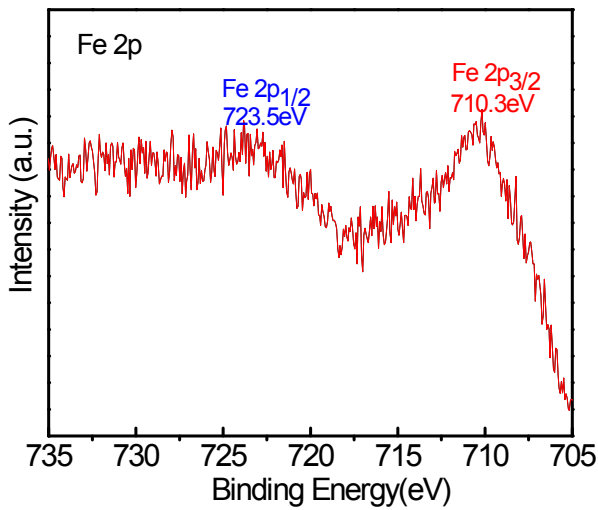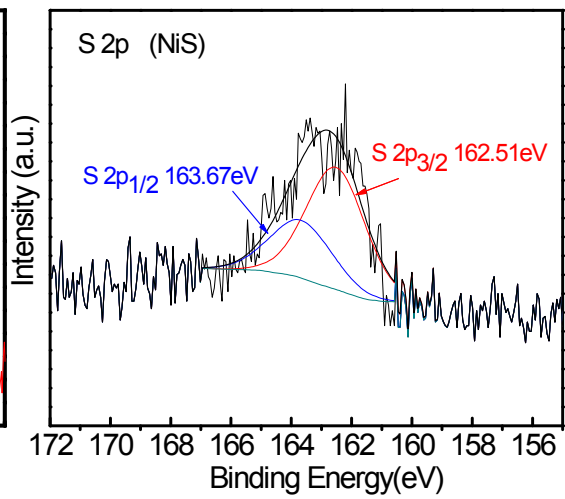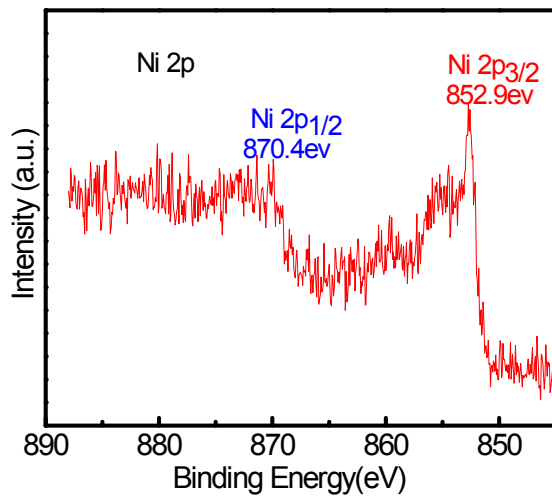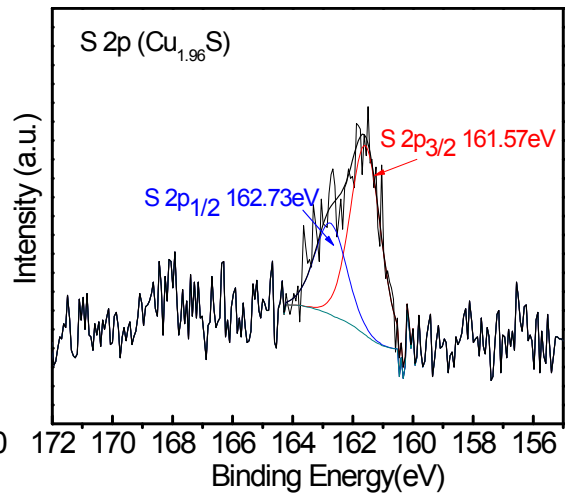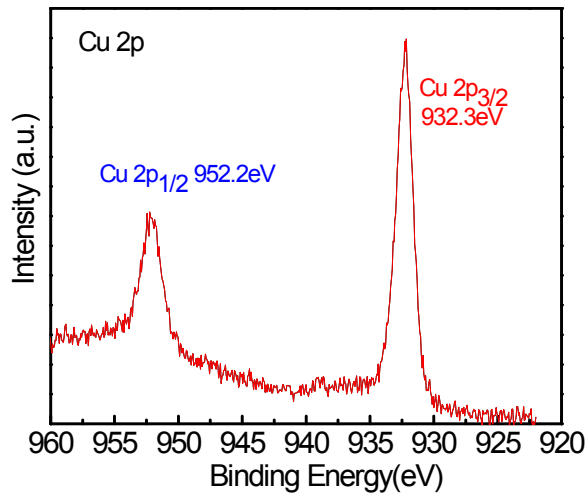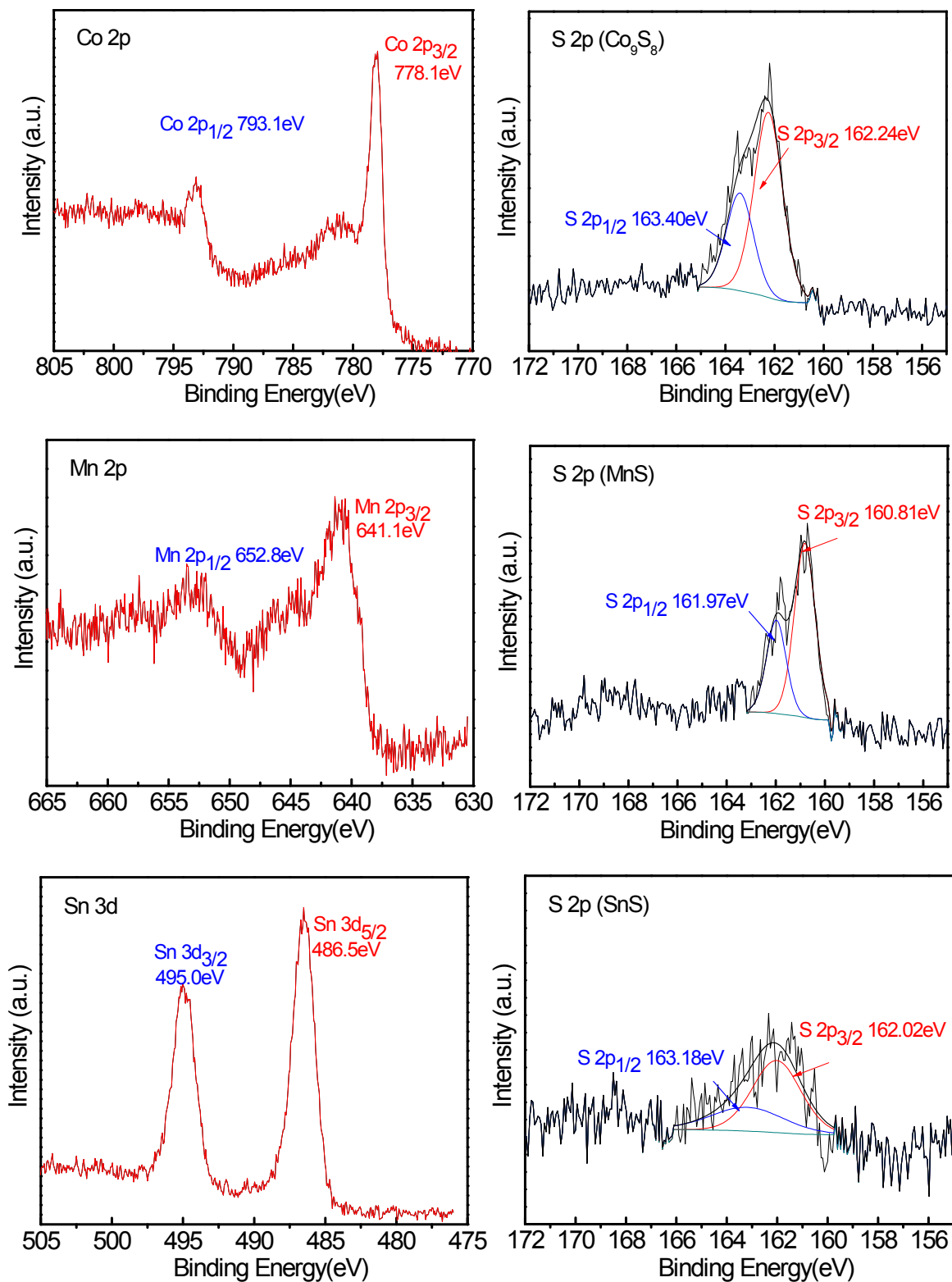
Figure S2 XPS core level spectra of metallic phase and sulfur for all samples.

TGA Analysis

TGA analysis was conducted. The process involved combustion of carbon, and redox reaction of metal sulfide with oxygen (Metal sulfide + Carbon nanofiber + Oxygen→ Metal oxide + Carbon dioxide + Sulfur dioxide). The mass loss (reading from Fig.S3)=mass of Sulfur+ mass of Carbon-mass of Oxygen in the final metal oxide(Co_3O_4, Mn_2O_3, Fe_2O_3, CuO, NiO, and SnO_2). Based on this formula, the calculated weight percentages of Co_9S_8, MnS, FeS, $Cu_{1.96}S$, NiS, and SnS in their composites are 32.8%, 27.8%, 31.5%, 28.8%, 36.4%, and 50.6%, respectively.
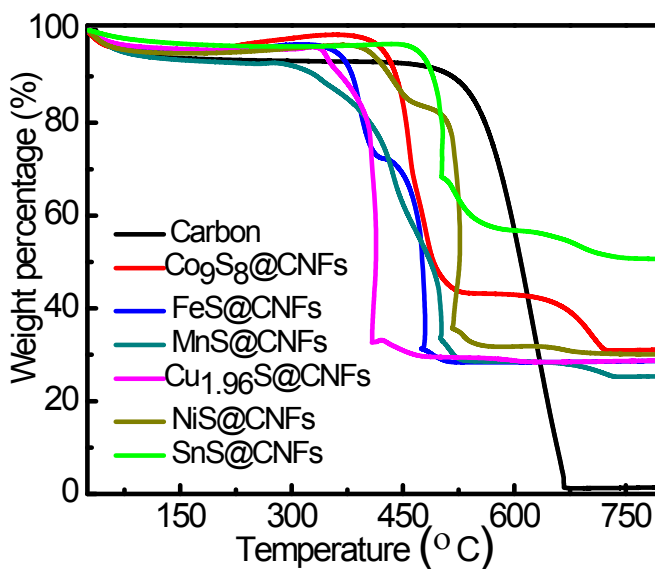

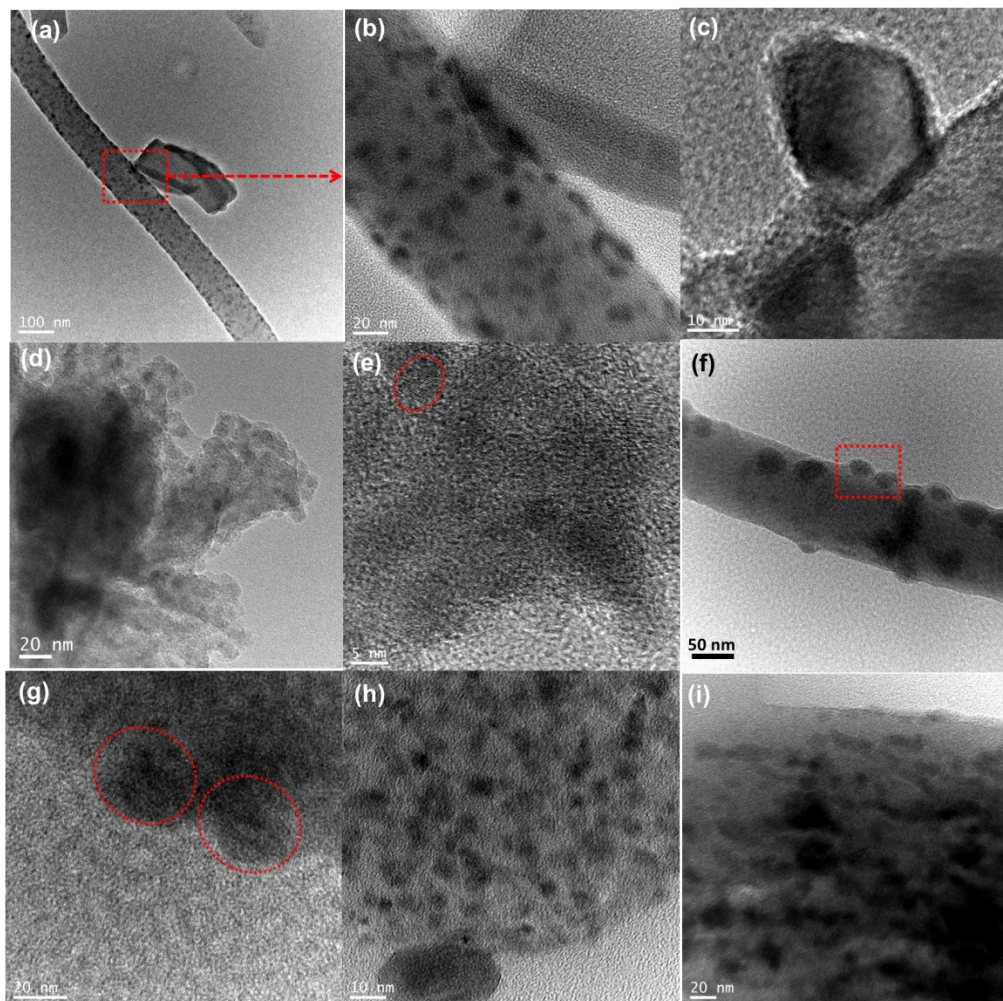**Figure S3** TGA analysis of all the samples in flowing air.

HRTEM

Figure S4 HRTEM of (a)&(b)$Cu_{1.96}S$@CNFs; (c)Co_9S_8@CNFs; (d)&(e)FeS@CNFs; (f)&(g)MnS@CNFs; (h)NiS@CNFs; (i)SnS@CNFs.

Cyclic Voltammetry Analysis

To investigate the electrochemical reactions taken place, all the first cycle charge-discharge profiles and their CV curves are provided and analyzed:

SnS: In the first cycle, the broad cathodic peak around 0.7V could be attributed to the formation of solid electrolyte interface layer (SEI) and reaction of lithium ions and SnS to form Li_2S and Sn. The sharp current increase below 0.2V represents the alloy reaction of Sn and Li ions. The

broad anodic peak around 0.7V indicates the dealloying reaction of Li-Sn. The broad cathodic peak around 1V in the following cycles is related to the partially reversible reaction of Li_2S, and the weak anodic peak around 2.1V indicates the formation of polysulfides. The first discharge curve shows a plateau around 1V, corresponding to the decomposition of SnS, plateau below 0.5V corresponds to SEI formation and alloying of Sn and Li. The two obscure plateaus around 0.7 and 2.0V in charge curve represent the dealloying reaction and delithiation of Li_2S. The observation is in accord with previous report.[6]

Other metal sulfides, different form alloying and dealloying reaction in SnS, have redox reaction with lithium ions.

$Cu_{1.96}S$: The peak around 0.4V in the first cycle could be the formation of SEI layers. The cathodic peaks around 1.5V and 2.05V indicate the insertion of lithium ions to the copper sulfide. The two anodic peaks (1.92V, 2.4V) correspond to the delithiation process. Both the cathodic and anodic peak pairs are in accordance with the sloping potential region in the charge and discharge curve. In addition, the cathodic peak around 0.2V observed after the 1st cycle and anodic peak around 0.5V should be the reaction between lithium and carbon nanofibers derived from PAN.[7] The appearance of the carbon peaks is due to the relatively low electrochemical activity of the $Cu_{1.96}S$, indicating by its low specific capacity.

MnS: the broad cathodic around 0.6V represents the reaction of MnS with Li ions to form Li_xMnS. The anodic around 1.5V can be assigned to reaction: $Li_xMnS+xe^- \leftrightarrow Mn+Li_xS, 0<x<2$). The first discharge and charge curve have plateau around 0.5V and 1.5V, representing the above mentioned reactions, respectively.

FeS, Co_9S_8, and NiS: The three metal elements are neighbors in periodic table, sharing lots of similarities. Their sulfides also show very similar electrochemical reaction with lithium ions. Their CV curves are very similar despite slight shifts of peak position and different peak density. The cathodic peaks around 0.9V for FeS ,Co_9S_8 and 0.75V for NiS in the first cycle represents the reaction with lithium to form lithium sulfide (Li_2S) and corresponding metallic phase (Fe, Co, Ni). This peak also exists in following curves although slightly shifted to the higher potential range. The reduction peaks around or below 0.5V are attributed to the formation of SEI. The anodic peak 2.1V comes from the reversible oxidation of metallic phase. The weak anodic curvature at ~1V in the first cycle possibly corresponds to the partial oxidation of the SEI.[8] It gradually disappears after the first cycle, indicating formation of stable SEI layer. The plateaus in the charge and discharge curves are in accord to CV peaks. The CV curve observed here is the same as those previously reported.[8,9]

It is also worth to point out that the subsequent scans almost overlap with each other in all the samples, suggesting excellent reversibility and structural stability of the electrodes.
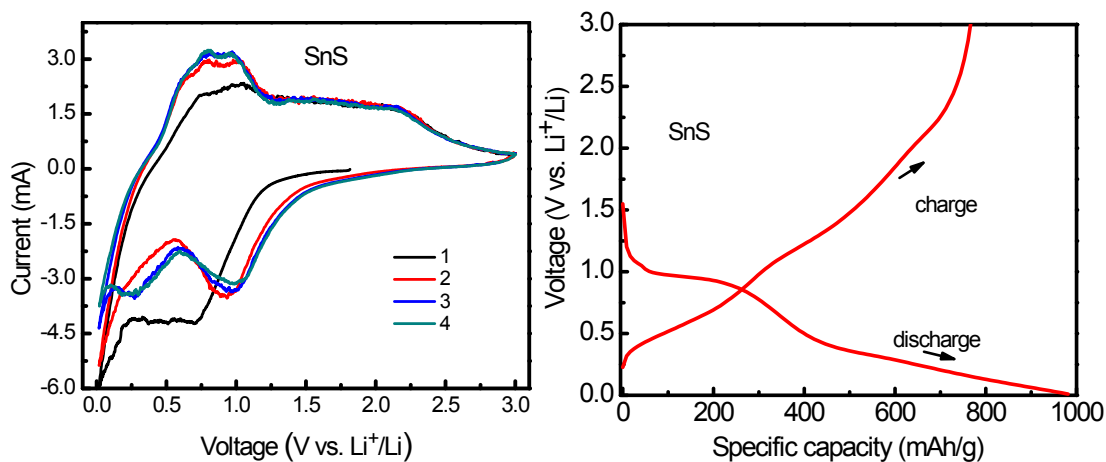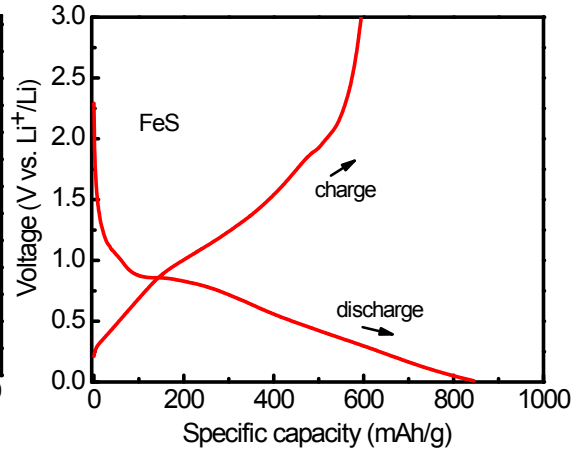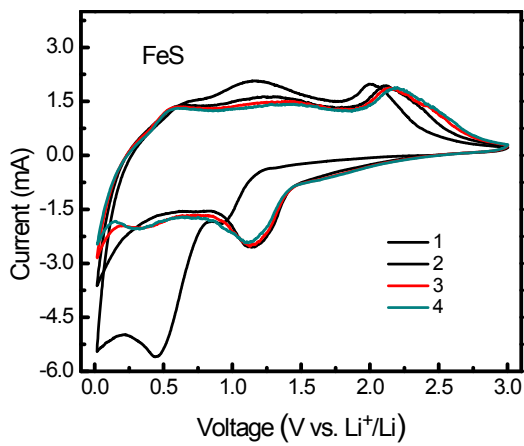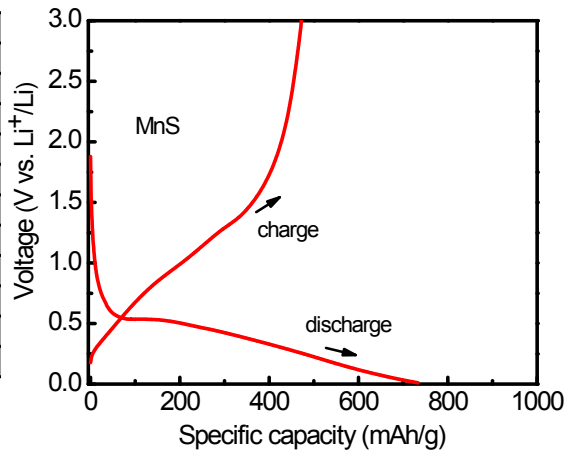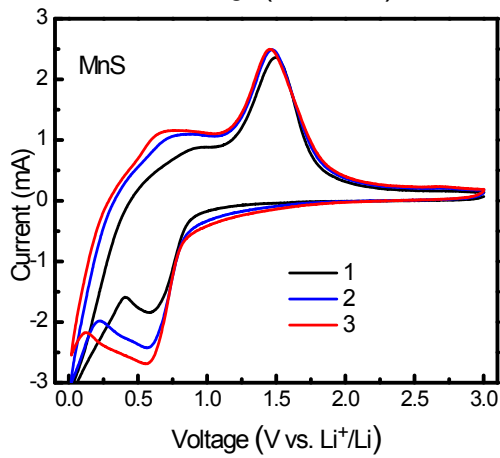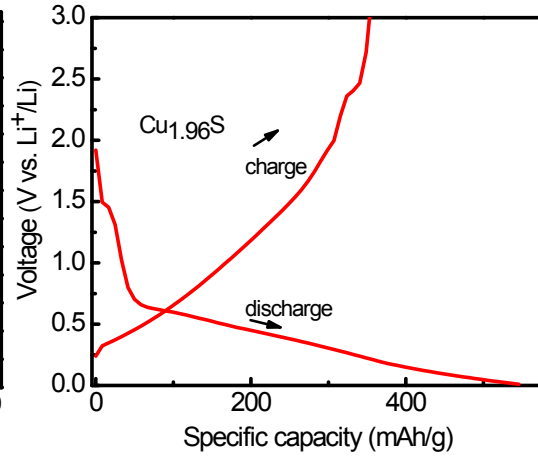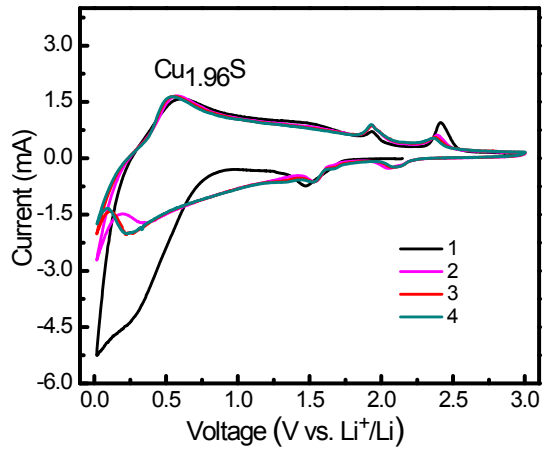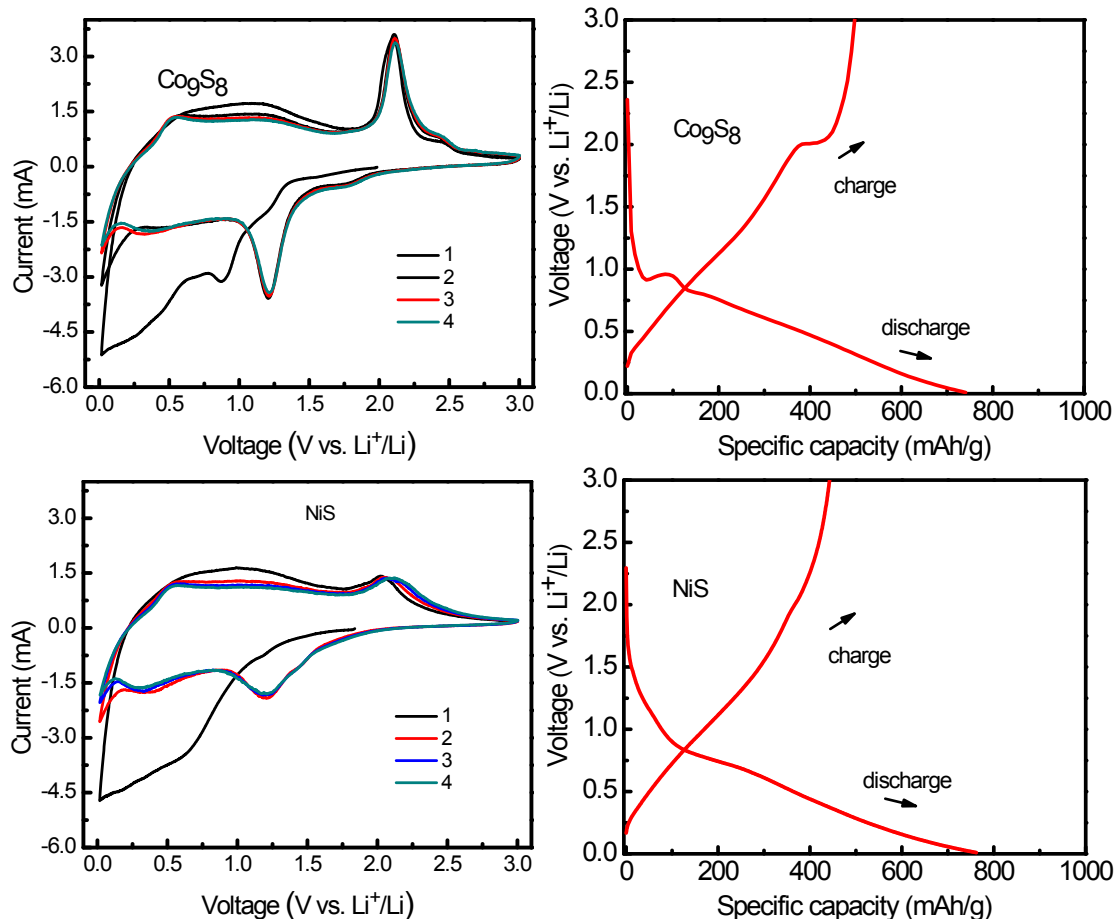
Figure S5 the voltage profiles and CV curves of all samples.

Reference

1 Z. Wang, L. Pan, H. Hu and S. Zhao, *CrystEngComm,* 2010, **12**, 1899

2 X. Wang, Q. Xiang, B. Liu , L. Wang , T. Luo , D. Chen and G. Shen, *Sci. Rep.*2013,**2007**,1.

3 K. Qi, R. Selvaraj, U. Jeong, S. Al-Kindy, M. Sillanp, Y. Kim and C. Taie, *RSC Adv.*, 2015, **5**, 9618.

4 G. Yue, Y. Lin, X. Wen, L. Wang, Y, Chen and D. Peng, *Appl. Phys. A*, 2012, **106**, 87.

5 A.Tang, S. Qu, K. Li, Y. Hou, F. Teng, J. Cao, Y. Wang and Z.Wang, *Nanotechnology*, 2010, **21**, 285602.

6 M. Zhang, D. Lei, X. Yu, L. Chen, Q. Li, Y. Wang, T. Wang and G. Cao, *J. Mater. Chem.,* 2012, **22**, 23091.

7 C. Chen, R. Agrawal, Y. Hao and C. Wang, *ECS J. Solid State Sci. Technol.,* 2013, **2**, M3074.

8 W. Shi, J. Zhu, X. Rui, X. Cao, C. Chen, H. Zhang, H. H. Hng and Q.Yan, *ACS Appl. Mater. Interfaces,* 2012, **4**, 2999.

9 Y. Zhou, D.Yan, H. Xu, S. Liu, J. Yang and Y. Qian, *Nanoscale,* 2015*,* **7***,* 3520.